



## Dynamic Modelling of the Gasification Region of a Bubbling Fluidized Bed Gasifier

Cláudio C. Oliveira\*, Jornandes D. da Silva

Polytechnic School - UPE, Environmental and Energetic Technology Laboratory; Rua Benfica - 455, Madalena, Recife - PE, Brazil. Cep: 50750-470  
[claudiothor@hotmail.com](mailto:claudiothor@hotmail.com)

This paper focuses on the dynamic mathematical model using algorithm of Runge-Kutta method Gill's method in predicting the process variables (temperatures and mole fractions of components "i" in the feed) in the gasification region for a bubbling fluidized bed coal gasifier. The discretized dynamic mathematical model has formed an ordinary differential equation (ODEs) system. The system of EDOs will be solved with the implementation of Runge-Kutta method Gill's method to examine the temperature behaviors of gaseous and solid phases as well as the mole fraction profiles for O<sub>2</sub>, CO, CO<sub>2</sub>, H<sub>2</sub>O, H<sub>2</sub> and C<sub>(s)</sub>. A model validation procedure was conducted to obtain by comparing the model confirmations using available data of the literature.

### 1. Introduction

The gasification is a thermochemical conversion process to produce, from carbonaceous fuel, a gas product with a useful heat value that can be applied as combustible gas or synthesis gas for later use. The thermochemical conversion modifies the chemical structure of solid combustibles through high temperature. The gasification agent enables that the feeding current be converted quickly into gas through different homogeneous and heterogeneous reactions (Ross et al., 2004).

The mathematical models for the gasification systems are important means to project such systems starting from a laboratory scale to industrial scale as well as starting from an existing system extrapolating them to condition one wants to use. A good model will help to identify the performance sensibility of a gasifier device through variation of different operation conditions and project parameters (Petersen and Werther, 2005).

The mathematical modelling can act in a significant way to explain the temperature behavior of the gas and solid phases in the gasification zone device of bubbling fluidized bed. To the current research, the equations of energy balance of both phases (gas and solid) were formed with the following restrictions: the equation for the gas phase involves the terms related to the thermal accumulation in the gas phase, thermal convection, thermal dispersion, gas-solid heat transfer, gas-wall heat transfer and chemical reaction rate of the homogeneous reactions. While the equation for the solid phase involves the referred terms of thermal accumulation in the solid phase, the thermal convection of the solid phase, the thermal dispersion of solid phase, solid-gas heat transfer, solid-wall heat transfer and chemical reaction rates of the heterogeneous reactions. On the other hand, equations of the included chemical species involve the referred terms to the accumulation of chemical species, the convection of chemical species, the dispersion of chemical species, mass transfer of chemical species and net rates of chemical species in the reactions considered for the process. Based on these hypotheses, it is possible to develop a simplified mathematical model to analyze the dynamic behavior of temperatures in the gas

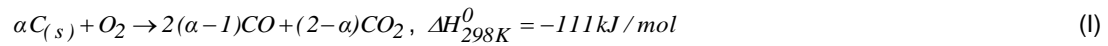
and solid phases and the chemical species that appear in the chemical reactions considered for the study (Silva, 2012).

The objective of this research is to analyze the temperature profiles ( $T_g$  and  $T_s$ ) as well as the profiles of mole fractions ( $Y_{O_2}$ ,  $Y_{CO}$ ,  $Y_{CO_2}$ ,  $Y_{H_2O}$ ,  $Y_{H_2}$  and  $C_{(s)}$ ) within the gasification region of the bubbling fluidized bed gasifier. In addition to, the model validation procedure was determined by comparing between the model for the gas temperature and Ross et al (2004). Similarly, the concentration for  $C_{CO}$  was also by means of comparing between the model in relation to  $C_{CO}$  and Petersen and Werther (2004).

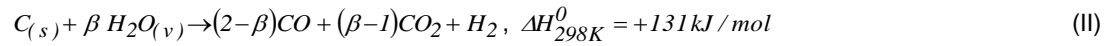
## 2. Kinetic mathematical models

The proposed process here is limited to two heterogeneous reactions that treat the combustion and gasification according to the procedure below. The chemical reactions chosen for this paper, resulting from the gasification region, involve carbon ( $C_{(s)}$ ), oxygen ( $O_2$ ), carbon monoxide (CO), carbon dioxide ( $CO_2$ ) hydrogen ( $H_2$ ) and water vapor ( $H_2O_{(v)}$ ). The two main chemical reactions in the gasification region are described by the following chemical equations as follows:

- combustion reaction



- carbon gasification



The reaction (I) is strongly exothermic, so the combustion reaction is favored by low temperature, while the reaction (II) is largely endothermic, therefore the carbon gasification reaction is benefited by high temperatures.

The reaction rate expressions developed by Petersen and Werther (2005) are used to describe the individual reaction rates. The intrinsic rates of these expressions are given as:

$$R_I = k_{r,1} CO_2 f(1) \quad (1)$$

$$R_{II} = \frac{K_{r,2} C_{H_2O} f(2)}{1 + K_{2,H_2O} C_{H_2O} + K_{2,H_2} C_{H_2} + K_{2,CO} C_{CO}} \quad (2)$$

Values of the various constants are summarized in Tables (1) and (2). For the expressions of  $k_{r,1}$ ,  $\alpha$ ,  $f_r$ ,  $K_{r,2}$ ,  $K_{2,H_2O}$ ,  $K_{2,H_2}$ , and  $K_{2,CO}$  see Tables (1) and (2).

The net rates of the various formation and consumption components  $I$ ,  $r_i$ , was then calculated by using Equations (1) and (2) as follows:

$$r_i = \sum_{j=1}^2 v_{ij} R_j, i = O_2, CO, CO_2, H_2O, H_2 \text{ and } C_{(s)} \quad (3)$$

Where  $v_{ij}$  is the stoichiometric coefficient of components  $i$ . If  $i$  refers to a reactant,  $v_{ij}$  is negative and for a product  $v_{ij}$  is positive. Thus, we have following net rates.

$$r_{O_2} = -R_I \quad (4)$$

$$r_{CO} = 2(\alpha - 1)R_I + (2 - \beta)R_{II} \quad (5)$$

$$r_{CO_2} = (2 - \alpha)R_I + (\beta - 1)R_{II} \quad (6)$$

$$r_{H_2O} = -\beta R_{II} \quad (7)$$

$$r_{H_2} = R_{II} \quad (8)$$

$$r_{C_{(s)}} = -\alpha R_{IC} - R_{IIC} \quad (9)$$

The intrinsic rates ( $R_I$  and  $R_{II}$ ) were introduced in Equations (3) to (7) to obtain the following Equations (net rates) of  $O_2$ , CO,  $CO_2$ ,  $H_2O$  and  $H_2$ .

$$r_{O_2} = -k_{r,1} C_{O_2} f_{(1)} \quad (10)$$

$$r_{CO} = 2(\alpha - 1) k_{r,1} C_{O_2} f_{(1)} + (2 - \beta) \frac{k_{r,2} C_{H_2O} f_{(2)}}{1 + K_{2,H_2O} C_{H_2O} + K_{2,H_2} C_{H_2} + K_{2,CO} C_{CO}} \quad (11)$$

$$r_{CO_2} = (2 - \alpha) k_{r,1} C_{O_2} f_{(1)} + (\beta - 1) \frac{k_{r,2} C_{H_2O} f_{(2)}}{1 + K_{2,H_2O} C_{H_2O} + K_{2,H_2} C_{H_2} + K_{2,CO} C_{CO}} \quad (12)$$

$$r_{H_2O} = -\beta \frac{k_{r,2} C_{H_2O} f_{(2)}}{1 + K_{2,H_2O} C_{H_2O} + K_{2,H_2} C_{H_2} + K_{2,CO} C_{CO}} \quad (13)$$

$$r_{H_2} = \frac{k_{r,2} C_{H_2O} f_{(2)}}{1 + K_{2,H_2O} C_{H_2O} + K_{2,H_2} C_{H_2} + K_{2,CO} C_{CO}} \quad (14)$$

Table 1: Kinetic parameters for the above equation (1)

$k_{r,1} = k_{r,0} \cdot \frac{T_s}{d_s} \exp\left(-\frac{E_{a,1}}{RT_s}\right)$	
$k_{r,0} = 3.574, \frac{m}{s.k}$ ; $E_{a,1} = 149,440, \frac{J}{mol}$	$f_r = 4.72 \times 10^{-3} \exp\left(-\frac{E_{a,2}}{RT_s}\right), \frac{J}{mol}$
$100\mu m \leq d_s (m) \leq 350\mu m$ ; $R = 8.3144, \frac{J}{mol.K}$ $E_{a,2} = 37.737, \frac{J}{mol}$ ; $f_{(1)} = 0.5$ ; $\alpha = \frac{1+2f_r}{1+f_r}$	

Table 2: Kinetic parameters for the above equation (2)

$k_{r,2} = k_{r,0} \cdot \frac{\rho_c}{M_c} (1 - X) \exp\left(-\frac{E_{a,3}}{RT_s}\right)$	$K_{(2),H_2O} = K_{(2,0),H_2O} \exp\left(-\frac{E_{a,4}}{RT_s}\right)$
$k_{r,0} = 2.39 \times 10^2, \frac{m^3}{mols}$ ; $E_{a,3} = 129.00, \frac{J}{mol}$	$K_{H_2O,0} = 3.16 \times 10^{-2}, \frac{m^3}{mol}$ ; $E_{a,4} = 30.100, \frac{J}{mol}$
$X = 0.05$ ; $f_{(2)} = 2.0$ ; $K_{(2),H_2} = K_{(2,0),H_2} \exp\left(-\frac{E_{a,5}}{RT_s}\right)$ ; $\beta = 1.2$ ; $K_{(2),CO} = K_{(2,0),CO} \exp\left(-\frac{E_{a,6}}{RT_s}\right)$	
$K_{H_2,0} = 5.16 \times 10^{-3}, \frac{m^3}{mol}$ ; $E_{a,5} = 59,800, \frac{J}{mol}$	$K_{CO,0} = 8.25 \times 10^{-5}, \frac{m^3}{mol}$ ; $E_{a,6} = 96.100, \frac{J}{mol}$

On the other hand, the intrinsic rate for  $C_{(s)}$  in chemical reactions (I) and (II) was given by  $r_{IC}$  and  $r_{IIC}$  as follows.

$$r_{IC} = \frac{6}{d_p} k_{diff} C_{O_2} \quad (15)$$

Where,

$$k_{diff} = \frac{Sh D_{O_2}}{d_p};$$

$$Sh = 2 \varepsilon_{g,mf}$$

$$r_{IIC} = 4.45 \exp\left(-\frac{E_a}{RT_s}\right) C_{H_2O}^{0.83} \varepsilon_s \quad (16)$$

Where,

$$E_a = 166.156 \text{ J/mol}$$

Equations (15) and (16) for  $r_{IC}$  and  $r_{iC}$  were placed in Equation (9) to obtain the net rate for  $C_{(s)}$  as follows.

$$r_{(s)} = -12\alpha \frac{\varepsilon_{g,mf}}{d_p^2} D_{O_2} C_{O_2} - 4.45 \exp\left(\frac{-E_a}{RT_s}\right) C_{H_2O}^{0.83} \varepsilon_s \quad (17)$$

### 3. Energy and mass balance equations for the gasification region

A non-isothermal mathematical model was developed to describe the gasification region process in the bubbling fluidized gasifier. The energy and mass balance equations were derived based on the assumptions given previous papers. For ideal gas, the simplified energy balance equations are given as follows.

- Balance of energy in the gas phase

$$\varepsilon_g C_{p,g} \rho_g \frac{\partial T_g}{\partial t} - \frac{4\varepsilon_g C_{p,g} \rho_g Q_g}{\pi d_c^2} \frac{\partial T_g}{\partial z} = \varepsilon_g K_g \frac{\partial^2 T_g}{\partial z^2} + h_{gs} S_{gs} (T_g - T_s) - \frac{4h_{sw}}{d_c} (T_g - T_w) \quad (18)$$

- Initial and contour conditions in the gas phase;

$$T_g|_{t=0} = T_{g,0}; K_g \frac{\partial T_g}{\partial z} \Big|_{z=0^+} = \frac{4C_{p,g} \rho_g Q_g}{\pi d_c^2} \left[ T_g \Big|_{z=0^+} - T_{g,0} \right]; \frac{\partial T_g}{\partial z} \Big|_{z=L^+} = 0 \quad (19)$$

- Balance of energy in the solid phase;

$$\varepsilon_s C_{p,s} \rho_s \frac{\partial T_s}{\partial t} + \frac{4\varepsilon_s C_{p,s} N_s \rho_s}{\pi d_c^2} \frac{\partial T_s}{\partial z} = \varepsilon_s K_s \frac{\partial^2 T_s}{\partial z^2} - h_{sg} S_p (T_s - T_g) - \frac{4h_{sw}}{d_c} (T_s - T_w) + \sum_{j=1}^{N_{rs}=2} (-\Delta H_{r,j}) R_{i,het} \quad (20)$$

Where,

$$\sum_{j=1}^{N_{rs}=2} (\pm \Delta H_{r,j}) R_{i,het} = (\Delta H_{r,I}) k_{r,I} C_{O_2} f(I) + \frac{(\Delta H_{r,II}) K_{r,2} C_{H_2O} f(2)}{1 + K_{2,H_2O} C_{H_2O} + K_{2,H_2} C_{H_2} + K_{2,CO} C_{CO}} \quad (21)$$

- Initial and contour conditions in the solid phase;

$$T_s|_{t=0} = T_{s,0}; K_s \frac{\partial T_s}{\partial z} \Big|_{z=0^+} = \frac{4\varepsilon_s N_s C_{p,s}}{\pi d_c^2} \left[ T_s \Big|_{z=0^+} - T_{s,0} \right]; \frac{\partial T_s}{\partial z} \Big|_{z=L^+} = 0 \quad (22)$$

For componet i, the simplified mass balance equations have been described by the following equations:

- Balance of mass for the chemical species;

$$\varepsilon_g \frac{\partial Y_i}{\partial t} + \varepsilon_g \frac{4Q_g}{\pi d_c^2} \frac{\partial Y_i}{\partial z} = \varepsilon_g D_i \frac{\partial^2 Y_i}{\partial z^2} + k_{gs} S_{gs} (Y_i - Y_c) + r_i; i = O_2, CO, CO_2, H_2O e H_2 \quad (23)$$

- Initial and contour conditions in the solid phase;

$$Y_i|_{t=0} = Y_{i,0}; D_i \frac{\partial Y_i}{\partial z} \Big|_{z=0^+} = \frac{4Q_g}{\pi d_c^2} \left[ Y_i \Big|_{z=0^+} - Y_{i,0} \right]; \frac{\partial Y_i}{\partial z} \Big|_{z=L^+} = 0 \quad (24)$$

The non-isothermal mathematical model involves a partial differential equation (PDEs) system in the axial and time domain (Equations 18 to 24). The axial domain of this PDEs system was discretized using a mixture of central finite difference, forward finite difference and backward finite difference to obtain an ordinary differential equation (ODEs) system. The ODEs system was solved the Runge-Kutta Gill's method for predicting the temperature behaviors within of gaseous and solid phases as well as the mole fraction behaviors for  $O_2$ ,  $CO$ ,  $CO_2$ ,  $H_2O$ ,  $H_2$  and  $C_{(s)}$ .

### 4. Results and discussions

The gasification region for bubbling fluidized bed gasifier was modelled to analyze the temperatures profiles within the gaseous and solid phases as well as the mole fraction profiles for  $O_2$ ,  $CO$ ,  $CO_2$ ,  $H_2O$ ,  $H_2$  and  $C_{(s)}$ . The physicochemical properties used in the numeral simulation are presented as follows:

gaseous void fraction  $\varepsilon_g = 0.41$ , gas specific heat capacity at constant pressure  $C_{p,g} = 1.092 \times 10^3 \text{ J kg}^{-1} \text{ K}^{-1}$ , gas density  $\rho_g = 0.456 \text{ kg m}^{-3}$ , gas flow  $Q_g = (9.87 \times 10^{-1} - 6.39 \times 10^{-5}) \text{ m}^3 \text{ s}^{-1}$ , diameter of the gasification region  $d_c = 0.10 \text{ m}$ , gas thermal conductivity  $K_g = 5.63 \times 10^{-2} \text{ W m}^{-1} \text{ K}^{-1}$ , gas-solid convective heat transfer coefficient  $h_{gs} = 8.41 \times 10^2 \text{ W m}^2 \text{ K}^{-1}$ , gas-solid specific area per unit volume of the gasification region  $S_{gs} = 4.372 \times 10^3 \text{ m}^2 \text{ m}^{-3}$ , gas-wall convective heat transfer coefficient  $h_{gw} = 1.85 \times 10^2 \text{ W m}^2 \text{ K}^{-1}$ , gas feed temperature  $T_{g,0} = 450 \text{ }^\circ\text{C}$ , solid feed temperature  $T_{s,0} = 470 \text{ }^\circ\text{C}$ , wall temperature  $T_w = 450 \text{ }^\circ\text{C}$ , solid void fraction  $\varepsilon_s = 0.63$ , coal specific heat capacity at constant pressure  $C_{p,s} = 1.101 \times 10^3 \text{ J kg}^{-1} \text{ K}^{-1}$ , particle density  $\rho_s = 2.50 \times 10^3 \text{ kg m}^{-3}$ , coal feed rate  $N_s = 0.334 \text{ kg h}^{-1}$ , coal thermal conductivity  $K_s = 7.13 \times 10^2 \text{ W m}^{-1} \text{ K}^{-1}$ , reaction heat of reaction (I)  $\Delta H_{r,I} (850^\circ\text{C}) = + 40.635 \text{ kJ mol}^{-1}$ , reaction heat of reaction (II)  $\Delta H_{r,II} (850 \text{ }^\circ\text{C K}) = + 429.311 \text{ kJ mol}^{-1}$ , reaction constant ( $k_{r,1}$ ) from the chemical reaction (I) is given in Table (1), reaction constant ( $k_{r,2}$ ) from the chemical reaction (II) is given in Table (2), adsorption constant ( $K_{(2), \text{H}_2\text{O}}$ ) is shown in Table (2), adsorption constant ( $K_{(2), \text{H}_2}$ ) is shown in Table (2), adsorption constant ( $K_{(2), \text{CO}}$ ) is shown in Table (2), diffusion coefficient of  $\text{O}_2$   $D_{\text{O}_2} = 2.021 \times 10^{-5} \text{ m}^2 \text{ s}^{-1}$ , diffusion coefficient of  $\text{CO}$   $D_{\text{CO}} = 1.801 \times 10^{-5} \text{ m}^2 \text{ s}^{-1}$ , diffusion coefficient of  $\text{CO}_2$   $D_{\text{CO}_2} = 1.381 \times 10^{-5} \text{ m}^2 \text{ s}^{-1}$ , diffusion coefficient of  $\text{H}_2\text{O}$   $D_{\text{H}_2\text{O}} = 2.178 \times 10^{-5} \text{ m}^2 \text{ s}^{-1}$ , diffusion coefficient of  $\text{H}_2$   $D_{\text{H}_2} = 4.126 \times 10^{-5} \text{ m}^2 \text{ s}^{-1}$ , diffusion coefficient of  $\text{C(s)}$   $D_{\text{C(s)}} = 1.718 \times 10^{-5} \text{ m}^2 \text{ s}^{-1}$  and gas-solid mass coefficient transfer  $k_{gs} = 1.812 \times 10^{-3} \text{ m}^3 \text{ s}^{-1}$ .

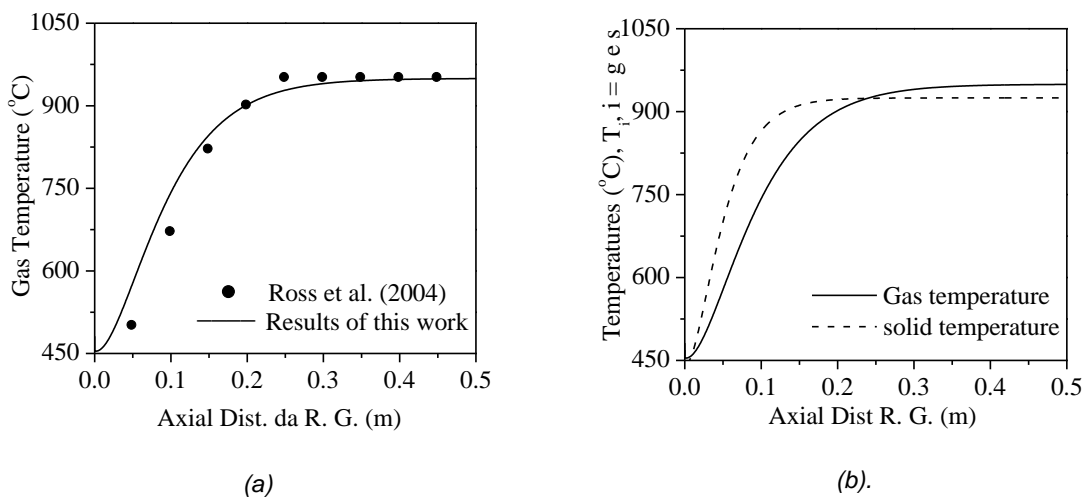


Figure 1: (a) Comparisons of predicted gas temperature profiles and Ross et al., (2004). (b) : Profiles of temperatures within of gas and solid in the gasification region versus axial distance (0.5 m) of the bubbling fluidized gasifier.

The Figure (1a) has shown by means of comparing a verification to validate the gas temperature using data of the literature. Since 0.26m the results of this work are acknowledged with the results established by Ross et al., (2004). The Figure (1b) shows the profiles for the temperatures within the gas and solid phases along the axial distance at the gasification region of the bubbling fluidized gasifier. After 0.2m the gas temperature exceeds the solid temperature.

The Figure (2c) represents a comparison between the results of this research and the results obtained of the literature for the concentration of CO. Thus, it was shown a good fit between our results and the results presented by Peterson and Werther (2005). The Figure (2d) presents the profiles of the mole fractions for  $\text{O}_2$ ,  $\text{CO}$ ,  $\text{CO}_2$ ,  $\text{H}_2\text{O}$ ,  $\text{H}_2$  and  $\text{C(s)}$ . After 0.35 m the chemical components ( $\text{O}_2$ ,  $\text{H}_2\text{O}$  and  $\text{C(s)}$ ) were totally consumed while the production in relation to other chemical components ( $\text{CO}$ ,  $\text{H}_2$  and  $\text{CO}$ ) follows the following condition:  $\text{CO}_2 < \text{H}_2 < \text{CO}$ .

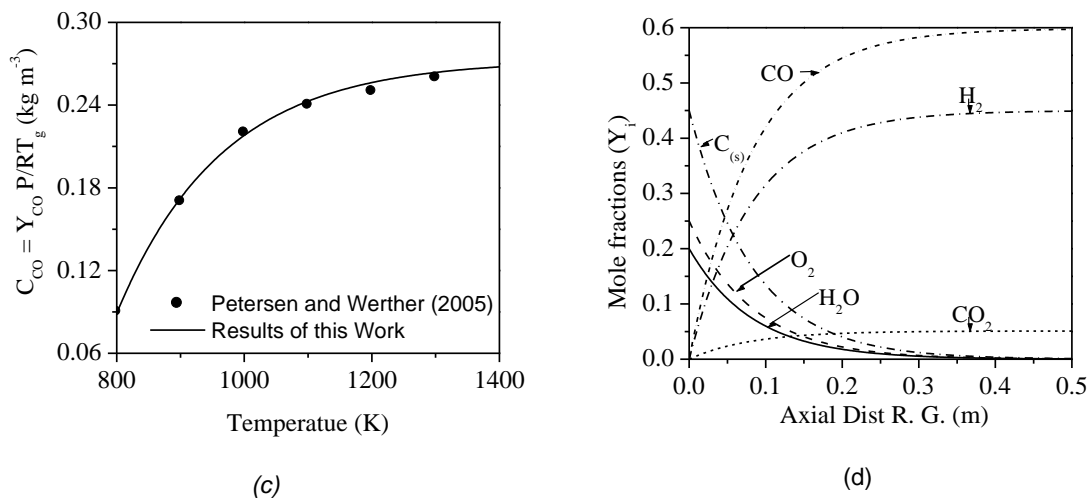


Figure 2: (c) Comparisons of predicted concentration profiles for CO and Petersen and Werther (2005) versus the gasifier temperature in the gasification region of the bubbling fluidized gasifier. (d) Profiles of mole fractions for chemical species ( $Y_{O_2}$ ,  $Y_{CO}$ ,  $Y_{CO_2}$ ,  $Y_{H_2O}$ ,  $Y_{H_2}$  and  $C_{(s)}$ ) within the gasification region of the bubbling fluidized bed gasifier.

## 5. Conclusions

The modelling of the gasification region at the bubbling fluidized bed gasifier was developed with respect to the temperatures ( $T_g$  and  $T_s$ ) as well as the mole fractions ( $Y_{O_2}$ ,  $Y_{CO}$ ,  $Y_{CO_2}$ ,  $Y_{H_2O}$ ,  $Y_{H_2}$  and  $C_{(s)}$ ) for the chemical species  $O_2$ ,  $CO$ ,  $CO_2$ ,  $H_2O$ ,  $H_2$  and  $C_{(s)}$ . The simulations for this model led us to the following conclusions:

- The validation retracted a satisfactory prognostication for the numerical experiment conducted for variables  $T_g$  and  $C_{CO}$ ;
- It was diagnosticated after 0.2m the gas temperature exceeds the solid temperature;
- It was Shown that chemical components ( $O_2$ ,  $H_2O$  and  $C_{(s)}$ ).

## Acknowledgements

The authors of this paper would like to thank CNPQ (National Council of Scientific and Technological Development) for the financial support given. (Process 483541/2007-9/Edict CNPq 15/2007 - Universal).

## References

- Petersen J., Werther J., 2005, Experimental investigation and modeling of gasification of sewage sludge in the circulating fluidized bed, *Chemical Engineering and Processing*, 44, 717-736.
- Ross D.P., Yan H., Zhang D., 2004, Modelling of a laboratory-scale bubbling fluidized bed gasifier with feeds of both char and propane. *Fuel*, 83(14), 1979–1990.
- Silva, J. D.;2012, Numerical Modelling of the Fluidynamics in a Bubbling Fluidized Bed Biomass Gasifier. *Journal of Petroleum and Gas Engineering*, 3, 35-40.